

Preparation of Combinatorial Arrays of Polymer Thin Films for Transmission Electron Microscopy Analysis

Kristen E. Roskov,^{1,†} Thomas H. Epps III,[‡] Brian C. Berry,^{§,†} Steven D. Hudson,[†] Maëva S. Tureau,[‡] and Michael J. Fasolka^{*,†}

Polymers Division, National Institute of Standards and Technology, Gaithersburg Maryland 20899, and Department of Chemical Engineering, University of Delaware, Newark, Delaware 19716

Received August 5, 2008

We present a new method for harvesting multiple thin film specimens from polymer combinatorial libraries for transmission electron microscopy (TEM) analysis. Such methods are of interest to researchers who wish to integrate TEM measurements into a combinatorial or high-throughput experimental workflow. Our technique employs poly(acrylic acid) plugs, sequestered in an elastomer gasket, to extract a series of film patches from gradient combinatorial libraries. A strategy for simultaneous deposition of the array of film specimens onto TEM grids also is described. We demonstrate our technique using nanostructured polymer thin film libraries as test cases in which the nanoscale details can be successfully imaged. Microscopy of test case specimens demonstrates that these samples are of sufficient quality for morphology screening via TEM, and in some cases are sufficient for more detailed morphological studies.

I. Introduction

Transmission electron microscopy (TEM) is an irreplaceable tool for characterization of a wide range of nanostructured materials and biological specimens. TEM provides, in many cases, nanoscale morphological information that cannot be easily achieved by other means; and because of its long history, data from TEM are readily understood. For these reasons researchers rely on TEM despite the fact that it can be a slow, tedious, and difficult technique. Accordingly, high-throughput or automated TEM specimen preparation and image collection capabilities are a very attractive research tool not only for practitioners of combinatorial materials research but also in industrial and clinical laboratories, where there is often a need to quickly characterize hundreds of specimens. However, there are serious technical barriers to constructing a high-throughput TEM workflow. The first set of challenges is related to TEM instrumentation design and operation. Because it is a high-vacuum instrument, TEM has a limited sample capacity, allowing for simultaneous loading of only one or two specimens, with several minutes for changing and introducing samples. Automatic focusing and tuning of TEM presents another difficulty because the optimal parameters are very sensitive to specimen type, position and tilt, and few instruments have integrated computer control and analysis. Recent years have seen progress in these respects. For example, there are reports in the literature on the design of multiple sample cartridges for TEM,^{1,2} and unpublished accounts from instrument vendors

indicate similar developments. In addition, the advent of TEM tomography measurements have resulted in strategies for automated tuning of instrument parameters and autofocus routines for TEM.^{3–8}

Preparation of appropriate specimen libraries is the other main challenge to high-throughput TEM and is the focus of this paper. TEM samples must be extremely thin (<100 nm), and thus, are difficult to create and manipulate in large numbers. Recently, focused ion beam (FIB) milling has been harnessed as a means for creating TEM specimens of “hard” materials, such as ceramics and metals.^{9,10} FIB enables fabrication of multiple samples from a combinatorial array, and a variety of complementary “lift out” techniques allow automated harvesting of these specimens.¹¹ As demonstrated, for example, by Chikyow and co-workers,¹² these methods are a promising route for high-throughput preparation of “hard” materials for TEM analysis.

For “soft” materials, such as polymers and biological specimens, progress toward high-throughput TEM analysis is less developed. For these systems, TEM specimen preparation is most often conducted via ultramicrotomy (or cryogenic ultramicrotomy) of bulk specimens, which is an inherently slow and “one-at-a-time” process. Indeed, published reports of automated or multispecimen ultramicrotomy are sparse.¹³ Other routes for TEM sample preparation are more promising with respect to combinatorial and high-throughput studies, especially if cast ultrathin films are the targets for analysis. For example, polymer thin films deposited on electron transparent silicon nitride substrates offer a suitable platform for TEM analysis,¹⁴ and this could potentially be harnessed for the characterization of combinatorial film arrays. However, the success of this method and other published techniques for polymer film lift off (e.g.,

* Corresponding author: mfasolka@nist.gov.

† National Institute of Standards and Technology.

‡ University of Delaware.

§ Current Address: Dept. of Chemical Engineering, North Carolina State University, Raleigh, NC 27695.

§ Current Address: Department of Chemistry, University of Arkansas at Little Rock, Little Rock, AR 72204.

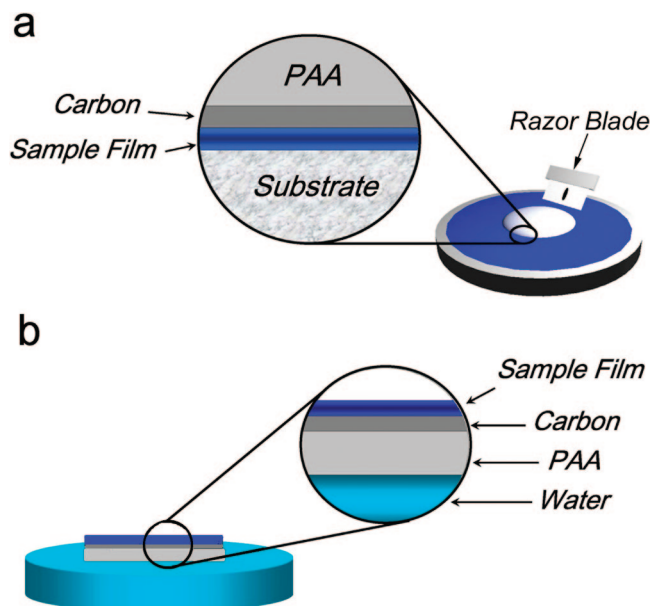


Figure 1. Schematic illustration of the peel off procedure for a single specimen. (a) A substrate-supported thin film sample coated with a thin layer of evaporated carbon (optional) and macroscopic layer of PAA solution. After the PAA is dried, the specimen is dislodged from the substrate with, for example, a razor blade (top right). (b) The PAA is dissolved on the surface of a pool of water. The floating film specimen is then retrieved on a TEM grid.

the use of sacrificial layers) typically depend on specific substrates.^{15,16}

In this paper, we describe and demonstrate a new method for the preparation of arrays of polymer specimens for TEM analysis. Our technique is well suited for harvesting large numbers of TEM specimens from continuous gradient and discrete combinatorial arrays of hydrophobic polymer thin films. As will be discussed below, this method addresses the practical problems of specimen fabrication and mounting in a highly parallel manner that can be easily scaled to hundreds of specimens. In principle, this technique does not seem strongly dependent upon the substrate employed or specimen processing (e.g., annealing), but as we will also discuss below, these factors can affect the adhesion between the substrate and polymer, which can adversely affect the quality of the harvested specimens.

II. Description of Procedure

Our combinatorial specimen preparation route leverages a “peel-off” technique previously reported by Fasolka et al.,¹⁷ which is based on published methods to produce carbon surface replicas for electron microscopy analysis.^{18,19} Figure 1 illustrates the key points of this procedure for a single specimen. First, a polymer film specimen is cast (via spin-coating or flow-coating) with a thickness appropriate for TEM, that is, below about 100 nm. There is flexibility in the choice of substrate material, as long as it is smooth, flat, and stiff; polished silicon wafers and glass microscope slides are excellent substrates. Optionally, the polymer film can be coated with a ~10 nm layer of evaporated carbon. The carbon layer’s function is either to protect the specimen through later steps if deemed necessary or act as a support against beam damage during TEM analysis; however, it is

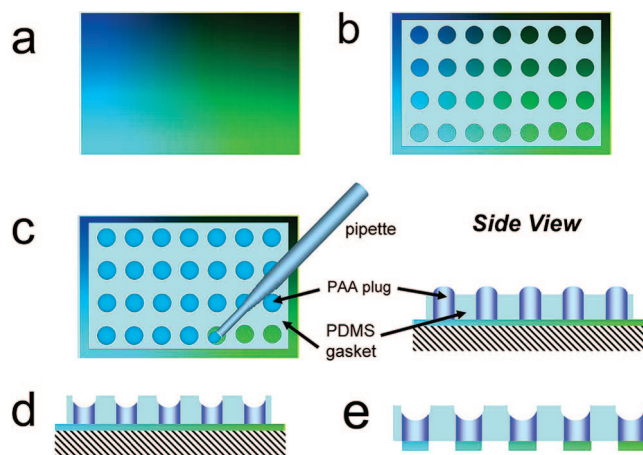


Figure 2. Schematic illustrations of the combinatorial peel off procedure. (a) Gradient thin film library on a flat, smooth stiff substrate (plan view). (b) Gradient film library with PDMS gasket in place. The gasket holes isolate specific library specimens. (c) Filling the gasket holes with PAA solution. Left: plan view. Right: cross-sectional view of one row of gasket holes. (d) Dried PAA plugs in gasket. (e) Immersion in liquid nitrogen results in film specimens attached to the bottom of PAA plugs embedded in the gasket.

not a critical step in the preparation of viable samples. Next, a 25% by mass aqueous solution of 250 kg/mol poly(acrylic acid) (PAA, Polysciences Inc., polydispersity index ≈ 2) is poured onto the specimen, enough to produce at least a 0.5 mm thick layer. The PAA solution is left to dry for 4–6 h until it is glassy and stiff. Mechanical peeling (e.g., with the edge of a razor blade), or immersion in liquid nitrogen then is used to dislodge the PAA layer from the substrate (Figure 1a). The detached PAA carries the film specimen (and carbon layer) with it intact. The specimen/PAA complex then is placed on a pool of deionized water (PAA side down) to dissolve the PAA, leaving a floating sample that can be retrieved with a TEM grid (Figure 1b).

As illustrated in Figure 2, our combinatorial version of the peel-off technique begins with the creation of an appropriate multivariate polymer library. For example, gradient fabrication techniques can create planar polymer libraries that continuously vary one or more factors including composition, film thickness, substrate surface energy, and processing temperature.^{20–25} A schematic two-dimensional gradient library is illustrated in Figure 2a. The thickness of these libraries is suitable for TEM analysis, and the library dimensions (typically a few centimeters on a side) are large enough such that a significant number of specimens can be extracted. The “sector spin-coating” technique, which creates pie-slice-shaped libraries of thin polymer films is another suitable fabrication route,²⁶ and it is possible that recent ink-jetting methods also may be appropriate.²⁷

The next step involves deposition of the PAA solution over the library. As illustrated in Figure 2b, an elastomer gasket (polydimethylsiloxane, PDMS) is placed over the library to isolate regions of interest for TEM analysis. To accommodate later steps described below, we use a 1 mm thick gasket with an array of 4 mm diameter holes arranged in the design of a standard 96 well plate (square array with 9 mm center-to-center spacing in both dimensions). In addition, one corner of the gasket is notched or otherwise marked so that its

orientation can be tracked through later steps. The gasket is used to sequester droplets or “plugs” of PAA solution deposited into the holes as shown in Figure 2c. For our example gasket, we deposit approximately 50 μL of PAA solution into each hole. This volume of solution represents about twice that of the gasket hole. Accordingly, when the 25% PAA solution dries, it will form a plug with a thickness of about half the hole depth. If deposited carefully, the PAA solution will form a neat dome over each hole (Figure 2c, right). In our work, solution deposition is achieved by hand with a pipet. However, this step could be automated using a robotic deposition system. Drying of the PAA solution (Figure 2d) is accelerated by placing the library in an oven heated to 40 $^{\circ}\text{C}$. Higher temperatures lead to unwanted cavitations and cracking in the PAA plug. Typical drying times are 6 h. The dry PAA plugs have a thickness of about 0.5 mm and a concave surface profile. We did not probe whether thinner PAA plugs are effective for film removal.

The dried library then is immersed in a bath of liquid nitrogen. Differential contraction between the PAA/specimen and the substrate causes patches of film below the PAA plugs to be pulled from the substrate. An audible “popping” sound indicates that pull-off has been achieved. Inspection of the gasket after it has been retrieved from the nitrogen pool reveals that the PAA plugs (with film specimens attached on them) remain lodged in the gasket holes, as illustrated in Figure 2e. This is critical because it ensures that the film samples retain their positional registry with respect to the original library. Bare circular patches on the library substrate indicate that films have been completely removed in these locations, while any partial or irregular patches indicate that pull off was not optimal in these locations.

As illustrated in Figure 3, the next phase of our procedure involves dissolution of the PAA plugs and deposition of the array of film specimens onto TEM grids. In these steps, we use a custom fabricated “basket array”, shown schematically in Figure 3a. The basket array consists of a rigid planar plastic gasket with a metal mesh adhered to one face. The plastic gasket holes have size and spacing equal to that of the PDMS gasket described in previous steps. In our studies, the mesh is a copper grid with square holes approximately 1 mm wide and spans approximately 200 mm wide (Buckbee-Mears). TEM grids (Ted Pella) are deposited into each “basket” of the array. Next, as shown in Figure 3b, the PDMS gasket (with embedded PAA plugs and samples) is placed on the basket array such that the holes between each gasket are registered, and the film samples are facing up. Then, the gaskets are placed in a shallow tank (e.g., a Petri dish) on top of 1 mm high spacers that elevate them from the tank floor (Figure 3c). The tank is filled, using a syringe, with deionized water until it is level with the top surface of the PDMS gasket, as illustrated in Figure 3d. The water flows into the gasket holes from below and makes contact with the PAA plugs. Water is introduced slowly enough that it does not upset the placement of the TEM grids in the basket array. Complete dissolution of the PAA takes approximately 6 h (see discussion below) and results in floating film specimens within each of the PDMS gasket holes. Next, the water is slowly withdrawn from the tank. In our study, water

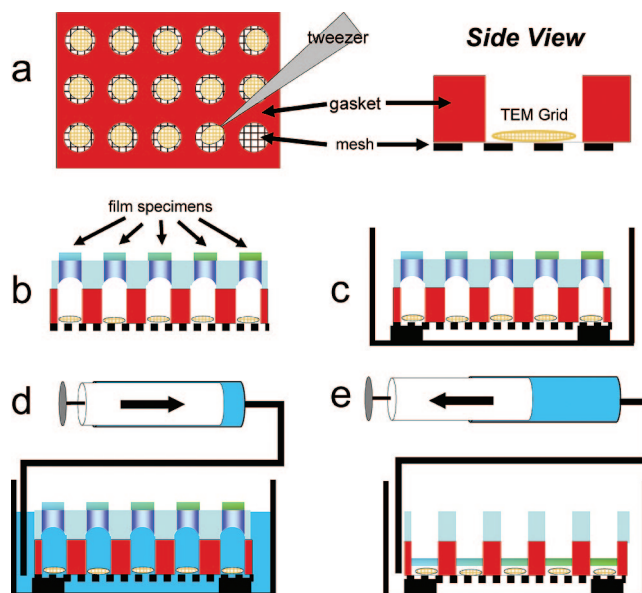


Figure 3. Schematic illustration of the specimen harvesting procedure. (a) Left: Plan view of basket array consisting of a plastic gasket with a metal mesh attached to one face. TEM grids are placed in the array. Right: Cross-sectional view of one “basket” with TEM grid in the bottom. (b) Cross-sectional view of stacked gaskets. The holes between each gasket are aligned and the film specimens face up. (c) Cross-sectional view of stacked gaskets in a shallow tank. Spacers elevate the stack 2 mm from the tank bottom. (d) The tank is filled with water to the top of the PDMS gasket. Water dissolves the PAA. (e) The water is withdrawn, depositing the film specimens on the TEM grids.

introduction and withdrawal is accomplished manually, but this step could easily be automated using a syringe pump. As the water level drops, the film specimens gradually lower until they settle on the TEM grids (Figure 3e). When all of the water has been removed, the TEM grids are retrieved, completing the process. Because the orientation and hole positions of the PDMS gasket are known, TEM data acquired from each of the array of specimens are correlated to their positions in the original combinatorial library.

III. Demonstration and Discussion

To demonstrate and test our method, we employed model thin film libraries. The first library consisted of a single block copolymer material exhibiting a gradient in film thickness. In addition, we tested the technique on a set of single-thickness specimens of three additional block copolymers species and a homopolymer/nanoparticle blend.

Thickness Library. The gradient thickness library consisted of a film of volume symmetric poly(styrene-*b*-2-vinylpyridine) [PS-*b*-PVP] block copolymer (50 kg/mol molecular mass, Polymer Source, Inc.) exhibiting a lamellar morphology. The gradient flow-coating technique²⁵ was used to deposit a continuous film thickness library onto a UV–ozone cleaned silicon wafer substrate with a native SiO₂ layer (n100 orientation, Virginia Semiconductor). Films were spread from a 3% by mass polymer solution in toluene resulting in a library that spanned a thickness range of 20–120 nm over a length of 80 mm. Film thicknesses were measured using UV–visible interferometry (Model F20, Filmetrics, Inc.). The library was annealed at 180 $^{\circ}\text{C}$ in

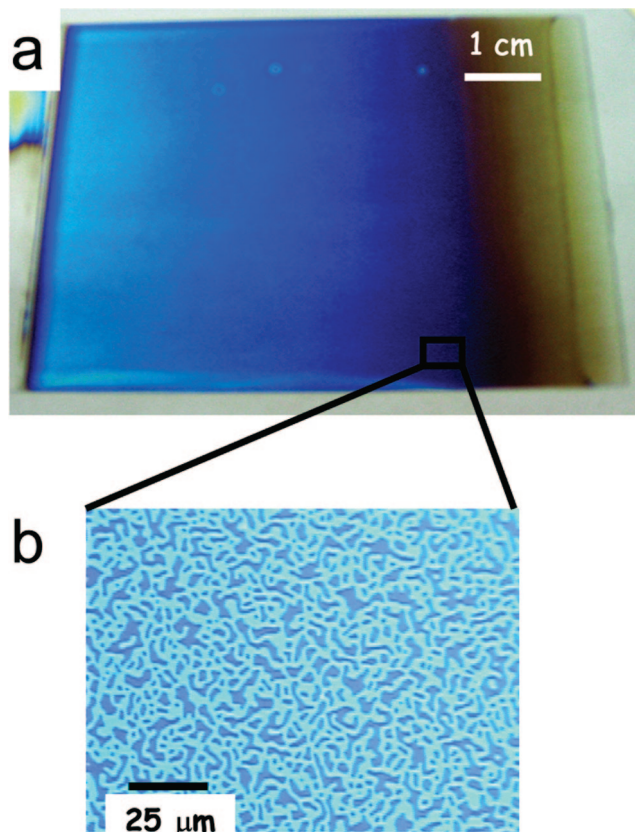


Figure 4. (a) Photograph of the block copolymer thin film library on a silicon wafer substrate. The film thickness increases from right to left. Hazy bands in the film indicate where the film surface has bifurcated into “island and hole” structures. (b) Detailed optical micrograph showing island and hole structures. Scale bar is approximate.

vacuum for 24 h to induce microphase separation of the block copolymer film. The digital photograph in Figure 4a shows the annealed film thickness library, with the film thickness increasing from right to left. In substrate-supported thin films, symmetric block copolymers exhibit a surface-directed lamellar morphology in which the lamellae are oriented parallel to the substrate surface.²⁸ Because of this effect, film thicknesses that accommodate an integral number of lamellar layers are stable and thus present a flat top surface. In all other cases, the top surface of the film bifurcates into discrete “island and hole” domains that take on the closest two stable film thicknesses. The digital photograph of the film library (shown in Figure 4b) illustrates this phenomenon, with alternating bands of hazy (bifurcated) and smooth (stable) films as the thickness increases.²² Optical microscopy (Nikon Optiphot II) of a hazy band, shows the discrete island and hole domains in detail. Observations of these structures will be discussed later.

Figure 5a shows our PS-*b*-PVP block copolymer film library with the PDMS gasket in place. This particular gasket accommodates 48 specimens. In this photograph, holes in the top half of the gasket have been filled with PAA solution. After the PAA was dried, the library was immersed in liquid nitrogen to detach specimens from the substrate. As shown in Figure 5b, an array of circular patches of exposed substrate demonstrates that all 48 specimens were successfully extracted from the library. For the library considered here, we

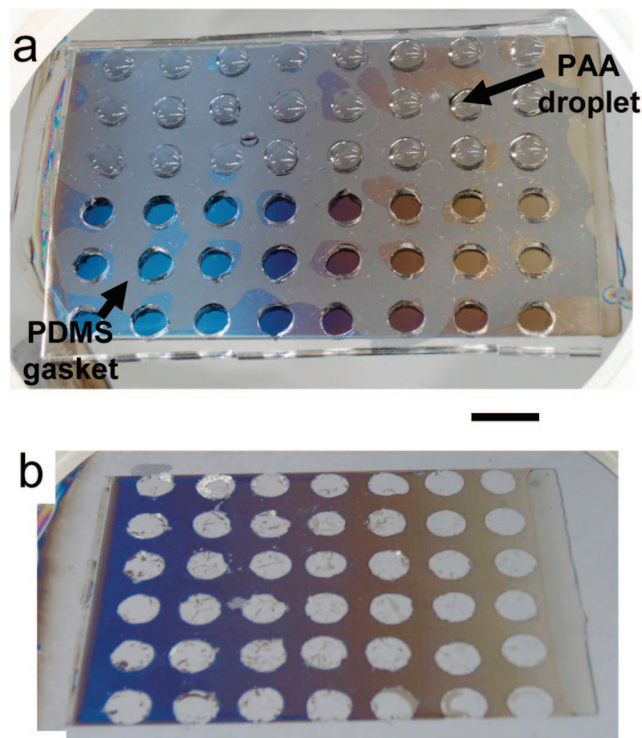


Figure 5. (a) Photograph of PDMS gasket on top of the thin film library. The top half of the gasket holes have been filled with PAA solution. (b) Photograph of library after specimen extraction. The array of circular patches of bare substrate indicates where specimens have been removed. Black scale bar (middle right) indicates ~1 cm.

verified film removal by performing atomic force microscopy (AFM) analysis of the edges of the circular patches. The hole depth measured by AFM matched the local film thickness as measured by interferometry, indicating that the entire film was pulled from the substrate. In addition, AFM micrographs in the middle of the holes revealed a smooth flat substrate, with no indication that film debris was left behind, as also observed via optical inspection. Surface spectroscopy techniques, such as X-ray photoelectron spectroscopy, could provide an automated means of determining whether full adhesive separation from the substrate occurred. As we discuss further below, in cases where film separation was incomplete, TEM images of the film specimens show tears and a fibrillar texture, and AFM analysis revealed fibrillar debris on the substrate after peeling. Since our test library exhibited a gradient in film thicknesses between 20 nm, and 120 nm, our demonstration also reveals that for this material our process works over the entire range of thicknesses that is relevant to TEM specimen preparation.

A custom-built basket array, shown in Figure 6a, was constructed by attaching a copper grid to one side of a stiff plastic gasket with double sided adhesive tape. The inset micrograph at the bottom right of Figure 6a shows TEM grids deposited into the basket array. Figure 6b shows the PDMS gasket (with embedded PAA plugs and film specimens) positioned over the basket array as illustrated in Figure 3b. The stacked gaskets were processed in a pool of deionized water to dissolve the PAA and deposit the films on TEM grids. Before the water was withdrawn, visual

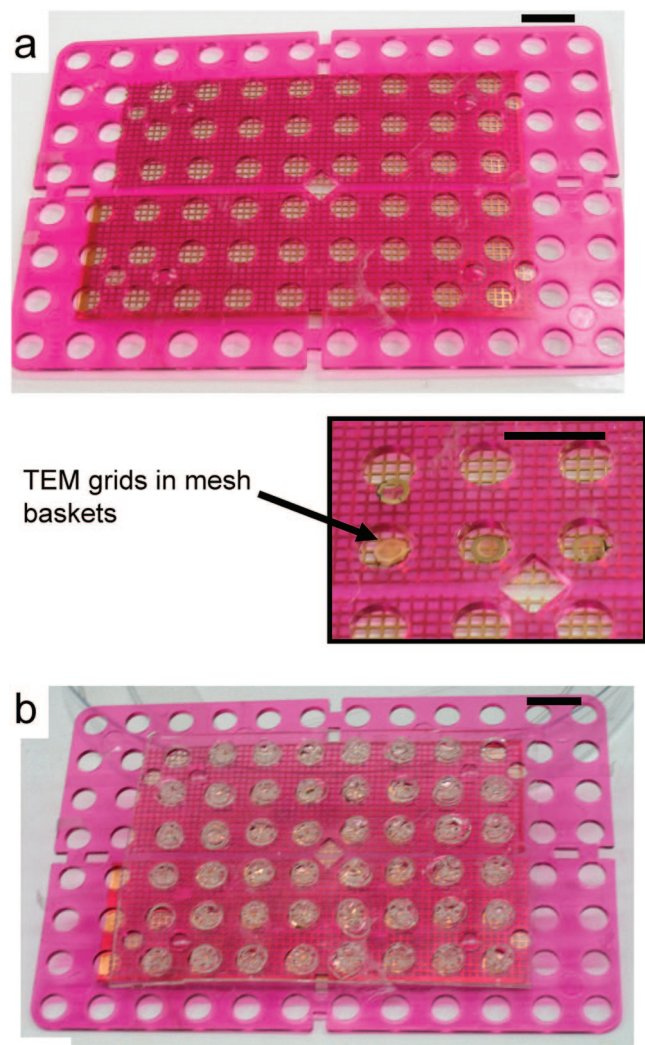


Figure 6. (a) Photograph of basket array constructed from a plastic gasket and a copper mesh. The inset (bottom right) shows TEM grids placed in the basket array. (b) Basket array with sample-loaded PDMS gasket stacked on top of it. Black scale bars in each photograph indicate ~ 1 cm.

inspection revealed a complete array of 48 floating films sequestered within the holes of the upper PDMS gasket.

After the water was removed, optical microscopy was used to assess whether suitable films were deposited onto the TEM grids. The criterion for success was that an unwrinkled block copolymer film large enough to acquire a TEM micrograph could be found on a grid. Figure 7 shows representative optical micrographs of TEM grids residing within the basket array mesh. The micrograph in Figure 7a shows a grid with no film deposited on it. In this image the larger spans behind the grid are part of the basket array mesh. Figure 7b shows a grid covered with a suspended film. In this reflection-mode optical image, the thin film specimen reflects the light, so the basket array mesh spans below the film cannot be seen. Because the suspended films can be easily detected with optical microscopy, it is simple to tell whether the specimen transfer was successful. Higher magnification optical images of these suspended films show the island and hole structures discussed above (Figures 7c and 7d). This indicates that the captured films consist of the block copolymer. Overall, 40 of the 48 grids exhibited specimens suitable for TEM analysis, and most of these grids were completely covered

with unwrinkled film. Microscopy examination of cases when specimens were not observed on the grids revealed that films had become pinned to the side of either the PDMS or plastic gaskets as water was withdrawn; these films did not lower onto the grids properly. The degree of successful specimen recovery can likely be improved by more careful construction of the gaskets to ensure that they do not have burs or rough areas to snag the film edges. Another possible solution is to fabricate the gaskets out of more hydrophobic materials, for example a fluoro-elastomer or poly(tetrafluoroethylene). Chemical modification of PDMS also may suffice for this purpose. Library designs that incorporate replicate specimens (like the 1-D thickness gradient library we examined) also can alleviate the impact of this problem if it occurs.

Finally, to establish the viability of harvested specimens for TEM analysis, randomly selected specimens were examined using a Phillips EM400T transmission electron microscope at an accelerating voltage of 120 kV. As shown in Figure 8, quality TEM micrographs were acquired from the specimens. These micrographs exhibit the island and hole structures discussed above. As illustrated in the schematic cross section in Figure 8b, the image contrast in the TEM micrographs (Figure 8c–d) develops due to the discrete domains of different thickness. While only a small fraction of the 40 harvested specimens were actually analyzed via TEM, the fact that island and hole structures were observed on every sample via optical microscopy strongly indicates that TEM would have been successful if attempted. In this respect, it should be noted that incompletely dissolved layers of PAA are typically visible via optical microscopy, and residual PAA usually renders the specimens too thick (a micrometer or more) to perform TEM. For specimens in this study, which were left on the water bath for over 6 h, no residual PAA was observed by either optical microscopy. However, this does not rule out the possibility that a uniform, ultrathin (few nanometers) film of PAA could remain adsorbed to the specimens. The presence of such a layer can be observed in TEM through a texture that develops as accumulated electron dose degrades the polymer. We did not observe this effect in our thoroughly washed films. It would be possible to detect a residual PAA layer using X-ray photoelectron spectroscopy or other surface sensitive methods, but we did not conduct such measurements.

Additional Materials. We further tested our method on four different polymer materials: (1) a nanocomposite material consisting of 1 wt % 5 nm CdSe quantum dots in a 25 000 g/mol poly(styrene) [PS] matrix, (2) a volume asymmetric poly(styrene-*b*-methyl methacrylate) [PS-*b*-PMMA] block copolymer (total molecular weight of 47 000 g/mol with $f_{PS} = 0.66$), (3) a volume asymmetric poly(styrene-*b*-isoprene) [PS-*b*-PI] block copolymer (total molecular weight of 43 000 g/mol with $f_{PS} = 0.72$), and (4) a volume asymmetric PS-*b*-PVP block copolymer (total MW of 34 000 g/mol with $f_{PS} = 0.69$). Each of these materials was cast into a 50 nm thick film strip, 2.5 cm wide and 7.5 cm long, using the flow coating technique describe above. The films were annealed in vacuum at 180 °C for 12 h to induce microphase separation (where applicable). Films 1 and 2 were examined on a Phillips EM400T transmission electron

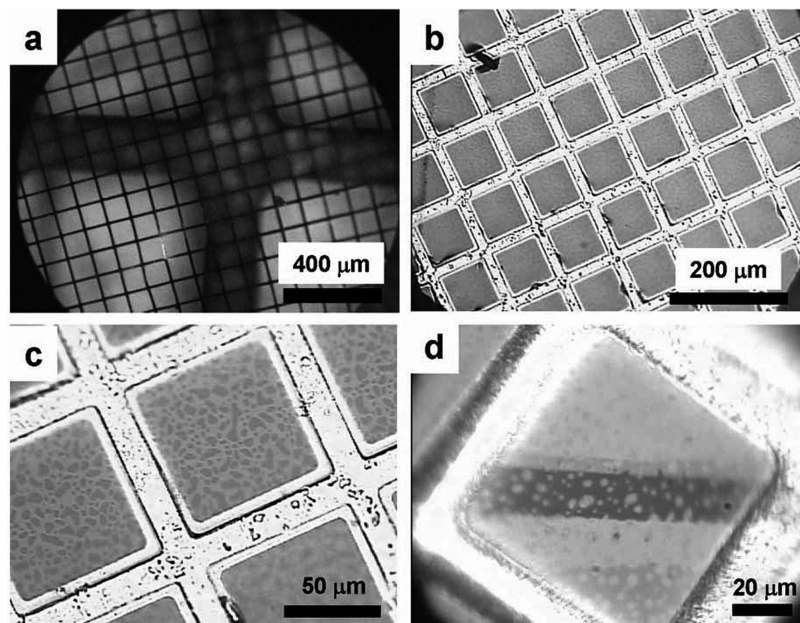


Figure 7. Optical micrograph showing the results of specimen deposition onto TEM grids. (a) Grid without specimen. The copper mesh is seen in the background. Eight of the 48 specimens did not have films. (b) Grid with representative film specimen. Forty of the 48 specimens exhibited smooth unwrinkled films suspended on the grid and suitable for TEM analysis. (c and d) Higher magnification micrographs reveal the island and hole structures that block copolymer films exhibit.

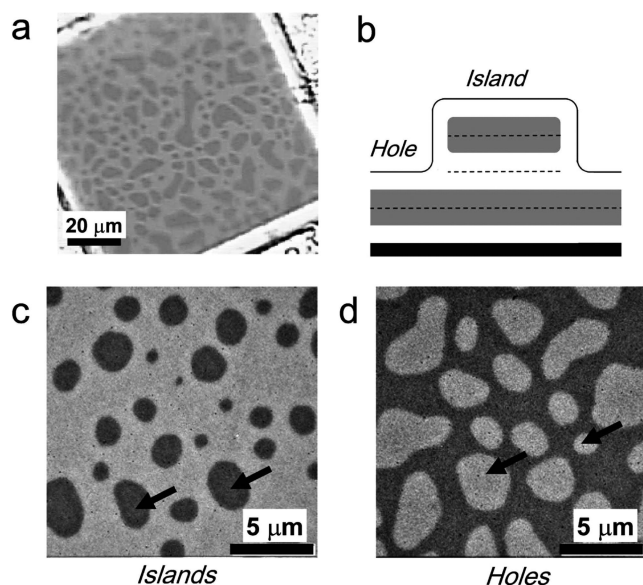


Figure 8. Testing the viability of the harvested film specimens for TEM analysis. (a) Optical micrograph of suspended film showing island and hole structures. (b) Schematic cross section of the film showing island region and hole region, the gray regions are polystyrene, white regions are poly(2-vinylpyridine). Thickness variations in the film cross-section are the cause of contrast in plan-view TEM micrographs. (c and d) Two representative TEM micrographs. The light regions are the thinner holes, and the dark regions are the thicker islands in the block copolymer film.

microscope at an accelerating voltage of 120 kV; films 3 and 4 were imaged on a JEOL JEM-2000FX transmission electron microscope operating at 200 kV. To test the efficacy of an intermediary carbon layer on the specimens, approximately half of each of the film strips the library were treated with ~ 10 nm of evaporated carbon. Then, the films were processed in an identical manner to the thickness library described previously.

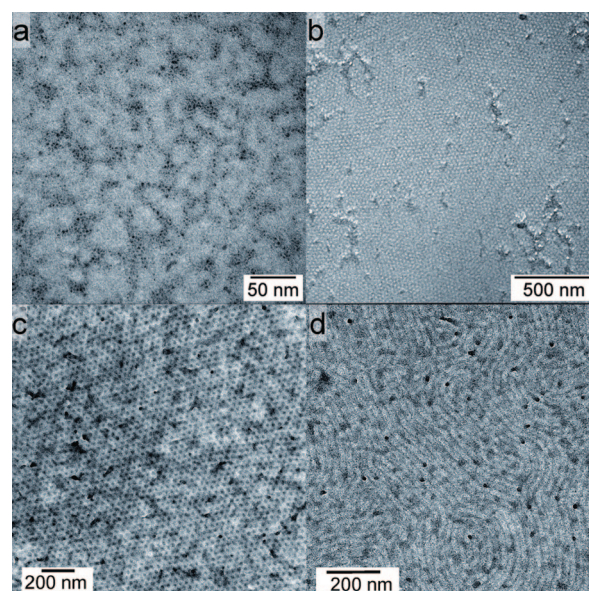


Figure 9. Representative TEM images from 4 film specimens peeled from silicon wafer substrates. All films were approximately 50 nm thick. (a) CdSe quantum dots in a PS matrix. (b) PS-*b*-PMMA block copolymer (c) PS-*b*-PI block copolymer stained with osmium tetroxide. (d) PS-*b*-PVP block copolymer stained with ruthenium tetroxide.

Figure 9 summarizes results from our second demonstration. The PS nanocomposite film was the most successful; Figure 9a shows a representative TEM micrograph obtained from these films. In this case, the films were removed cleanly from the substrate and high-quality TEM images of the inorganic particles could be obtained. High-quality images also were obtained from PS-*b*-PMMA, films. However, as seen in Figure 9b, there were qualitatively more rips and tears in the film than in the PS nanocomposite film, indicating that in these areas portions of the film were left behind on the substrate. For this material, introduction of a 10 nm thick film of evaporated carbon seemed to ease film removal,

leading to higher quality TEM images. We propose that the carbon acts as an adhesion promoter between the PAA and PS, which resides at the free surface of the film. This enhanced adhesion helps the PAA pull the PS-*b*-PMMA block copolymer intact from the substrate.

For the PS-*b*-PI and PS-*b*-PVP specimens, the results were less ideal because portions of the film were left behind. This is evident in Figure 9c, which shows a TEM micrograph of a PS-*b*-PI film specimen. In this image, the microphase-separated morphology of the block copolymer is clearly evident, but a fibrillar morphology indicative of a ductile film fracture from the surface also is observed (i.e., a craze viewed normal to its surface). Indeed, in this case, through atomic force microscopy analysis, residual fibrillar material could also be observed on the substrate following sample removal. The quality of the PS-*b*-PI specimens was not significantly improved by carbon deposition. As shown in Figure 9d, the PS-*b*-PVP specimen exhibited similar behavior. Film tearing is evident; however, the nanoscale morphological details remain clear.

The relative poor performance of the PS-*b*-PI as compared to the PS nanocomposite and PS-*b*-PMMA may be the result of the differences in glass transition temperatures (T_g) between these specimens. It is likely that the high- T_g PS and PS-*b*-PMMA polymers more easily undergo brittle adhesive fracture from the substrate surface, while the materials with low- T_g components, like PS-*b*-PI, are more likely to fracture in a cohesive manner under cryogenic shock.

A comparison of the PS-*b*-PVP and PS-*b*-PMMA illuminates the effect of film–substrate adhesion on the specimen removal process. While the PMMA and PVP have similar glass transition temperatures and stiffness, the PVP adheres to silicon oxide surfaces more strongly. Moreover, while addition of the carbon layer assisted removal of the PS-*b*-PMMA specimen, we observed no change in the quality of PS-*b*-PVP specimens when a carbon film was applied. This observation suggests that differential adhesion, that is, relative adhesion between the PAA and the film (modified by carbon) and between the film and the substrate, plays a substantial role in film removal. Accordingly, it may be possible to enhance the range of polymer specimens for which our method is useful by engineering the adhesion at each of these interfaces. As discussed previously, carbon increased the adhesion between some of our specimens and the PAA, and it is possible that thin intermediary layers of other materials could serve a similar purpose. Modification of the substrate, perhaps through treatment via a hydrophobic self-assembled monolayer, would tend to decrease adhesion between oxide substrates and strongly interacting polymers and thus improve film removal. However, we note that for block-copolymer and other polymers, changes in the substrate chemistry may affect the morphology of the specimen, which may not be desired.

Modification of the film processing route could also improve the ability of this method to handle more difficult film specimens. We note that the PAA/specimen “pops-off” under liquid nitrogen because of an abrupt differential contraction caused by rapid cooling and dramatic differences in the coefficients of thermal expansion between the polymers

and the silicon substrate. Accordingly, if a contraction-induced force threshold for PAA removal is reached before the sample material drops below its T_g , the system will be more likely to fail within the specimen resulting in incomplete film removal. It may be possible to overcome this limitation in softer, low- T_g specimens by slowly precooling the system to a temperature below the T_g of the sample and then plunging the system into liquid nitrogen for a stage of more rapid cooling.

IV. Conclusions

We described and demonstrated a new method for preparing arrays of TEM specimens from thin film libraries. The technique leverages a peel-off method to extract multiple patches of films from the specimen library. A parallel strategy for depositing the samples onto TEM grids also was described; in our demonstration 40 of the 48 specimens were retrieved simultaneously.

Our study employed several polymer thin films as demonstration cases. In addition, our method can be used with film libraries of polymer blends and nanocomposites (i.e., nanoparticle-filled systems). We demonstrated some of these possibilities directly through our second demonstration cases, and other reports show that peeling of “single” samples of blend and particle laden materials has been accomplished.²⁸ Published works also indicate that films can be peeled from topographically structured substrates,^{17,28} such as lithographic surfaces, and that peeled films can be further processed via microtomy for cross-sectional TEM analysis.¹⁷ In addition, this technique has potential for the analysis of the buried polymer/substrate interface, through, for example surface sensitive measurements like X-ray photoelectron spectroscopy.²⁹ In this study, the parallel technique worked best for glassy materials with T_g values above room temperature that have weak adhesion with the substrate. In these cases, we were able to obtain TEM micrographs with clear morphological details and without obscuring features that result from ductile fracture of the film. In specimens containing low- T_g materials or more substantial substrate adhesion, incomplete film removal and ductile fracture occurred, although the morphological details were still readily apparent. It is possible that results in such specimens could be improved by engineering the adhesion between the film and substrate or the film and the PAA or by modifying the film processing as discussed above. Finally, we note that the procedure described herein is not applicable to specimens that have strongly hydrophilic or water soluble components because interaction of the film with aqueous solutions may influence the nanostructure in samples with mobile water-sensitive moieties.

Our demonstration considered at most 48 specimens, but there is no reason why the process could not be scaled up to hundreds of specimens. This could be accomplished by either increasing the dimensions of the library (and gaskets, etc.) or by increasing the gasket hole density. The former approach will fail when the sample becomes too large for practical immersion in liquid nitrogen. The latter strategy will be limited by the mechanical reliability of

the gasket material between holes, and by the ability of small PAA plugs to effectively remove films from the substrate. From our observations, 1 mm sample areas spaced at 1 mm are feasible.

Acknowledgment. The authors thank Alamgir Karim and for helpful discussions. B.C.B. was supported by a National Research Council Postdoctoral Fellowship. K.E.R. was supported by the NIST SURF Program. This research made use of facilities at the NIST Combinatorial Methods Center (www.nist.gov/combi). The authors also made use of the W.M. Keck Microscopy Facility at the University of Delaware. **Disclaimer:** Certain commercial equipment, instruments, or materials are identified in this paper to specify the experimental procedure adequately. Such identification does not imply endorsement by the National Institute of Standards and Technology nor is it intended to imply that the materials or equipment identified are necessarily the best available for the purpose.

References and Notes

- (1) Lefman, J.; Morrison, R.; Subramaniam, S. *Biophys. J.* **2005**, *88*, 148A.
- (2) Morrison, R.; Subramaniam, S. *Biophys. J.* **2004**, *86*, 80A.
- (3) Dierksen, K.; Typke, D.; Hegerl, R.; Baumeister, W. *Ultramicroscopy* **1993**, *49*, 109–120.
- (4) Dierksen, K.; Typke, D.; Hegerl, R.; Koster, A. J.; Baumeister, W. *Ultramicroscopy* **1992**, *40*, 71–87.
- (5) Koster, A. J.; Deruijter, W. J. *Inst. Phys. Conf. Ser.* **1988**, 83–84.
- (6) Koster, A. J.; Deruijter, W. J. *Ultramicroscopy* **1992**, *40*, 89–107.
- (7) Koster, A. J.; Deruijter, W. J.; Vandenbos, A.; Vandermast, K. D. *Ultramicroscopy* **1989**, *27*, 251–272.
- (8) van der Laak, J. A. W. M.; Dijkman, H. B. P. M.; Pahlplatz, M. M. M. *Ultramicroscopy* **2006**, *106*, 255–260.
- (9) Overwijk, M. H. F.; Vandenheuvel, F. C.; Bulleieuwma, C. W. T. *J. Vac. Sci. Technol. B* **1993**, *11*, 2021–2024.
- (10) Phaneuf, M. W. *Micron* **1999**, *30*, 277–288.
- (11) Giannuzzi, L. A.; Stevie, F. A. *Micron* **1999**, *30*, 197–204.
- (12) Chikyow, T.; Ahmet, P.; Nakajima, K.; Koida, T.; Takakura, M.; Yoshimoto, M.; Koinuma, H. *Appl. Surf. Sci.* **2002**, *189*, 284–291.
- (13) Chiriboga, L.; Zhao, Y.; Wei, J. J.; Melamed, J. *J. Histotechnol.* **2005**, *28*, 245–248.
- (14) Morkved, T. L.; Lu, M.; Urbas, A. M.; Ehrichs, E. E.; Jaeger, H. M.; Mansky, P.; Russell, T. P. *Science* **1996**, *273*, 931–933.
- (15) Heier, J.; Genzer, J.; Kramer, E. J.; Bates, F. S.; Walheim, S.; Krausch, G. *J. Chem. Phys.* **1999**, *111*, 11101–11110.
- (16) Li, Z.; Qu, S.; Rafailovich, M. H.; Sokolov, J.; Tolan, M.; Turner, M. S.; Wang, J.; Schwarz, S. A.; Lorenz, H.; Kotthaus, J. P. *Macromolecules* **1997**, *30*, 8410–8419.
- (17) Fasolka, M. J.; Harris, D. J.; Mayes, A. M.; Yoon, M.; Mochrie, S. G. *J. Phys. Rev. Lett.* **1997**, *79*, 3018–3021.
- (18) Bassett, D. C. *Phil. Mag.* **1961**, *6*, 1053.
- (19) Geil, P. H. *Polymer Single Crystals*; Wiley Interscience: New York, 1963.
- (20) Meredith, J. C.; Karim, A.; Amis, E. J. *Macromolecules* **2000**, *33*, 5760–5762.
- (21) Meredith, J. C.; Karim, A.; Amis, E. J. *MRS Bull.* **2002**, *27*, 330–335.
- (22) Smith, A. P.; Douglas, J. F.; Meredith, J. C.; Amis, E. J.; Karim, A. *Phys. Rev. Lett.* **2001**, *87*, 015503.
- (23) Julthongpiput, D.; Fasolka, M. J.; Zhang, W. H.; Nguyen, T.; Amis, E. J. *Nano Lett.* **2005**, *5*, 1535–1540.
- (24) Sehgal, A.; Karim, A.; Stafford, C. F.; Fasolka, M. J. *Microsc. Today* **2003**, 26.
- (25) Stafford, C. M.; Roskov, K. E.; Epps, T. H.; Fasolka, M. J. *Rev. Sci. Instrum.* **2006**, *77*, 023908.
- (26) de Gans, B. J.; Wijnans, S.; Woutes, D.; Schubert, U. S. *J. Comb. Chem.* **2005**, *7*, 952–957.
- (27) Meier, M. A. R.; Schubert, U. S. *Soft Matter* **2006**, *2*, 371–376.
- (28) Fasolka, M. J.; Mayes, A. M. *Annu. Rev. Mater. Res.* **2001**, *31*, 323–355.
- (29) Epps, T. H.; Delongchamp, D. M.; Fasolka, M. J.; Fischer, D. A.; Jablonski, E. L. *Langmuir* **2007**, *23*, 3355–3362.

CC8001348